Solid-state SiO2 nano-gears AFM tip manipulation on HOPG

Jianshu Yang, Jie Deng, Cédric Troadec, Thierry Ondarçuhu, Christian Joachim

Solid-state SiO_2 nano-gears AFM tip manipulation on HOPG

Jianshu Yang[1,3], Jie Deng[2], Cedic Troadec[2], Thierry Ondarçuhu[1], and Christian Joachim[1,2,3]

[1]Nanoscience Group & MANA satellite, CEMES/CNRS, 29 Rue Marvig,
BP 94347, 31055 Toulouse Cedex, France

[2] Institute of Materials Research and Engineering,
A*STAR, 3 Research Link, 117602, Singapore

[3]International Center for Materials Nanoarchitectonics (MANA), National Institute for Materials Science (NIMS), 1-1 Namiki, Tsukuba, Ibaraki 305-0044, Japan

NANO-103815

In press, Nanotechnology, Nov. 2014

Abstract :

On a native graphite surface, 15 nm thick solid state nanogears are nanofabricated with an outer diameter down to 30 nm and 6 teeth. In a tapping mode, the nanogears are manipulated one at a time by the tip of an atomic force microscope using the sample stage displacements for the manipulation to construct mechanism like a long nanogears train. In absence of a central shaft per nanogear, gearing between nanogears is limited to a few 1/12 turns for 6 teeth. For step height below 3.0 nm, nanogears are manipulated up and down native graphite surface step edges. When the step is higher than 3 nm, a rack and pinion mechanism was constructed along a graphite step edge with a 90 nm nanogear pinion.

1. Introduction

Solid state gears are widely used in various mechanical machineries [1]. They are currently micro-fabricated down to the micron scale [2, 3, 4]. Following the work by Y.J. Yun and co-workers on solid state gear miniaturization below 1 □m [5, 6], we have miniaturized solid state gears by reporting the nanofabrication of amorphous SiO_2 nanogears down to 60 nm in diameter with a 30 nm thickness [7]. Those diameter and thickness are not compatible with the prospect of interconnecting mechanically a solid state nanogear with a single molecule-gear or a single molecule-motor [8,10].

In this paper, we present the nanofabrication of solid state SiO_2 nanogears down to 30 nm in diameter with a 15 nm thickness on flat highly ordered pyrolytic graphite (HOPG) terraces. Aside from this diameter reduction, one important aspect of this new process is the reduction of the nanogear thickness down to 15 nm with also the objective to explore the limit of solid state classical mechanics [9]. In a first section, our new process is presented approaching the nanogear thickness limit by a systematic exploration of the resist deposition conditions. In section 2, atomic force microscope (AFM) tip manipulations of the nanogears are presented in air with the recording of the characteristics AFM signals during a manipulation sequence (tapping mode oscillations amplitude, cantilever deflection). In section 3, some nanogears mechanics are presented. On the HOPG surface, we demonstrate that a native 10 graphene layers step edge height is required to play the role of a nanoscale rack for a 15 nm thick nanogear. Further developments of this work are presented in conclusion.

2. The nanogear fabrication process

In our initial hydrogen silsesquioxane (HSQ) nanogears fabrication process on a silicon surface [7], an intermediate Au layer was introduced between the HSQ layer and the silicon surface. This layer was important to chemically release the nanogears from the surface. Without this sacrificial layer, it was extremely difficult to manipulate a single nanogear using a scanning tunneling microscope (STM) or an AFM tip, even after hardening the HSQ gears by annealing the sample [7]. For the new process presented in this section, an HOPG surface was selected

with the objective to avoid those friction and anchoring effects. In effect and on HOPG, there is no need for an intermediate layer between HSQ and the HOPG surface, making the nanofabrication process simple and clean in view of future ultra-high vacuum (UHV) applications. In the following, the nanogears are fabricated out of a negative tone e-beam resist. The HSQ resist is directly spin coated on the HOPG surface. Our new and very simple process flow is presented in Fig. 1a. A freshly peeled-off HOPG surface was spin-coated with an HSQ resist (XR1541 from Dow Corning, 4000 rotation per minute) and baked at 90 °C for 5 min. Then, the HSQ / HOPG sample was e-beam exposed at a line dose of 0.48 nC/cm with a commercial ELS-7000 (Elionix) e-beam nanolithography system using an e-beam acceleration voltage of 100 kV and a current intensity of 50 pA. The exposed samples were developed in MF CD-26 (Shipley) for 60 seconds, then washed out with 1:9 CD-26 to de-ionized (DI) water for 10 seconds and finally rinsed in DI water during 30 seconds.

The fabricated HSQ nanogears were directly observed on the HOPG surface and first imaged using a high resolution scanning electron microscope (SEM). Fig. 1b shows a regular array of HSQ nanogears with an outer diameter ranging from 150 nm to 30 nm. The Fig. 2a SEM zoomed image is presenting two lines of five nanogears. On the ELS-7000, the diameter of the nanogear and the number of teeth was varied. For a 15 nm minimum thickness (see the discussion below), the smallest 30 nm in diameter nanogears obtained have 6 teeth and each tooth width is about 8 nm, the minimum observed with this process. Tapping mode AFM images of the same HOPG surface location confirm the 15 nm ± 1 nm thickness of the HSQ nanogears (see the profile line Fig. 2b). The smallest nanogears are often found not aligned on HOPG as compared with the e-beam mask indicating a weak surface interaction between the nanogears and the HOPG surface. In an AFM tapping mode and in SEM images, native steps of different heights (mostly 1 nm / 3 ML to 3.3 nm / 10 ML) can normally be found on the freshly cleaved HOPG surface depending on how the HOPG was peeled off. As presented in Fig. 2, our process preserves those steps edge because the end cleaning of the process was very well optimized and that AFM scanning in a tapping mode was used, avoiding any eventual manipulation and accumulation of surface residues. This was also confirmed by SEM images after the process.

It was also important to explore the HSQ resist thickness limits of our process in view of the possible use of solid state nanogears to transfer motion from / to a molecule-gear whose chemical structure height will not be larger than a few nm [10]. For this purpose, a defined

nanogear e-beam pattern with various nanogear diameters from 30 nm to 150 nm was used with different HSQ layer thicknesses. This thickness was varied from 15 to 90 nm by changing only the HSQ concentration. With a 1% HSQ solution, a uniform 15 nm thick HSQ film can still been obtained on HOPG. Concentrations lower than 1% results in non-uniform HSQ films with many pin-holes indicating a de-wetting of HSQ on the HOPG surface. Following this procedure, the HSQ nanogears were SEM imaged and their sizes systematically measured. Fig. 3a is presenting the variation of the smallest size nanogears obtained (outer diameter) as a function of the HSQ resist layer thickness. For a given HSQ layer thickness, the smallest nanogears were selected when at least a 1:1 ratio is reached between the teeth length and the teeth width. Below this 1:1 ratio, deformed or incomplete nanogears were not considered for Fig. 3. With a 15 nm thick HSQ layer, the smallest solid nanogears have an outer diameter of 30 nm with 6 teeth (each about 8 nm in width) as illustrated in Fig. 3b. For example, with an HSQ layer thicker than 50 nm, the smallest nanogear was about 60 nm in outer diameter.

3. Single solid state nanogear AFM tip manipulation

The small interaction between a nanogear and the HOPG surface opens the possibility to manipulate a nanogear one at a time and with an AFM tip in air. To reduce the piezo delay effects and the compensation which occurs when using single tube scanners to scan the surface over large distances, the nanogear manipulations were performed by scanning the sample stage instead of scanning the AFM tip. For this purpose, the HOPG sample was mounted on a XYZ piezo-controlled nano-positioning table (positioning error $\Delta < 2$ nm) inserted under a Dimension 3000 Bruker AFM head [11]. In this configuration, the AFM tip is used to push on the selected nanogear by moving the sample stage. Fig. 4 presents a 90 nm nanogear manipulated on an HOPG terrace. Here, a fresh nanogear (previously un-manipulated) was firstly selected using a tapping mode AFM image recorded in standard conditions, the other imaged nanogears being used as reference during the manipulation sequence. For a manipulation in a pushing mode, the tip apex was positioned about 60 nm away from the selected nanogear (marked by a cross on Fig. 4a). The manipulation starts by disengaging the AFM feedback loop and by a 10 nm tip apex approach towards the surface. Then, the piezo table is moved in the X direction for about 80 nm. In Fig. 4a, the initial set point voltage of the oscillation amplitude is 1.22 V (corresponding to a 27.3 nm oscillation amplitude). After pushing on the nanogear, the AFM feedback loop is turned on in normal tapping mode imaging conditions and the table brought back to its initial position. In Fig. 4b, the recorded AFM image

demonstrates that the selected nanogear had been moved by 40 nm to the left with a very small apparent clockwise rotation. After this first manipulation, Fig. 4c reports a second identical manipulation sequence also in a pushing mode over 50 nm with now no apparent rotation during the manipulation.

For nanogears between 57 nm and 153 nm in diameter (SEM measured) and following the above manipulation protocol, hundreds of single nanogear manipulations were performed demonstrating a 70% success of manipulating a nanogear by moving the sample stage. Below a diameter of 57 nm, AFM tip manipulations were not reproducible. This may be due to the tip apex used, not sharp enough in this case. Another observation is that after a first manipulation of a 90 nm fresh nanogear, the following manipulations require to start with only a 6 nm initial tip apex vertical displacement. This implies that after the nanofabrication process, the fresh 90 nm nanogears are still anchored on the HOPG surface.

The manipulation sequence from images Fig. 4a to 4b was analyzed by recording in time and during the manipulation sequence, the variations of the AFM cantilever oscillations amplitude and deflection (Fig. 4d and 4e). Instead of converting the timeline in sample stage displacements, the experimental timing was kept for the abscise in Fig. 4d and 4e showing also the manipulation signal during a short period of time before and after the starting of the manipulation sequence itself.

The solid line signal Fig. 4d is giving the time dependent variation of the cantilever oscillation amplitude during the first Fig. 4a to Fig. 4b manipulation of a fresh nanogear. From times T1 to T2, the tip scanning was stopped and the AFM feedback loop disengaged. As expected, the chosen 1.22 V (23.7 nm) oscillation amplitude voltage remains constant during this time interval. At time T2, this amplitude decreases abruptly to 0.6 V (13.4 nm) because the tip apex was approached to the surface by 10 nm. After this approach, the piezo table was moved 80 nm to the right for the tip apex to approach the nanogear by its edge and between two teeth. The amplitude remains at 0.6 V (13.4 nm) until time T3 where the nanogears and the tip apex start to interact. From T3 to T4, this interaction gradually increases up to time T4 where the AFM tip apex is touching the nanogear edge and starts to push resulting in a zero value of the oscillation amplitude signal. Then, the piezo table was moved to the right up to time T5. Here, the oscillation amplitude signal remains at zero volts for a few seconds more indicating that the nanogear and the tip apex are still in interaction long after stopping the piezo table. From Fig.

4b to 4c, the same time dependent signal was recorded during a second manipulation of the same nanogear. The starting oscillation amplitude is slightly higher in voltage (1.62 V). Notice that during this manipulation sequence, the time dependent signal is similar to the one recorded during the first manipulation.

To get more insights on the manipulation mechanisms, the cantilever deflection signal was also recorded with a voltage sensitivity of 1 mV per 0.165 nm of deflection. The time dependent solid line signal Fig. 4e corresponds to the first manipulation sequence from Fig 4a to Fig. 4b and the dashed line to the second one from Fig. 4b to Fig. 4c. The T1, T2, T3, T4 and T5 time markers are positioned following Fig. 4d. From T1 to T2, the cantilever deflection is almost constant since it is free to oscillate. The same deflection is also observed from T3 to T4 since the 10 nm vertical tip approach to the surface was just chosen to be in the range of the nanogear thickness. At time T4, the tip apex is touching the nanogear edge. Here, the deflection signal is characteristics of a quasi-stick-slip motion behavior during the follow up manipulation [12, 13]. With an intensity of 2 mV, the first large maximum (larger than the other up and down quasi-regular deflection features) indicates that the static friction is higher than the kinetic one. The cantilever alternatively bend up and down during this manipulation sequence. At time T5, the piezo table was stopped leading to a cancellation of the large oscillations. However, the average deflection does not return to its T1 value indicating that the cantilever is still bent down and the tip apex still interacting with the nanogear.

For the second manipulation from Fig. 4b to 4c, the time dependent dash curve deflection signal in Fig. 4e is similar to the first one with a notable small intensity of the first large initial deflection maximum at the beginning of the manipulation. This is indicative of a smaller static friction for this second manipulation as compared to the first one which was performed on a fresh nanogear. Notice as already discussed that it is difficult to manipulate a fresh nanogear without a little rotation along the manipulation pathway. After the first manipulation and by selecting a good tip apex location around the nanogear, a translation without rotation is possible. This confirms that the freshly nanofabricated nanogears are anchored on the HOPG surface. This may come from the nanofabrication process residues like non-polymerized HSQ remaining or because the HSQ polymerization step leads to an anchoring of the nanogears on HOPG surface native defects [14, 15, 16].

The two other possible sliding and pulling modes of manipulation have also been explored. A sliding mode is possible by positioning the tip apex on top of a nanogear and exerting a gentle pressure before moving the piezo table. Generally, this leads to very irregular stick-slip motions of the nanogear and consequently to a non-precise positioning. After approaching the tip apex to a nanogear as performed in Fig. 4 but now by the left, it was not possible to pull the nanogear by moving the piezo table.

Series of single nanogear manipulations were also performed for different tip apex heights while the tip apex was step by step approached towards the HOPG surface. The recording of this kind of manipulation signals is well known for single atom or molecule STM manipulations [17, 18]. As presented in Fig.5b and 5c, the oscillation amplitude of the cantilever and its deflection were simultaneously recorded as a function of the piezo table displacement. On those figures, z = 0 corresponds to the reference tip apex height before disabling the AFM feedback loop (corresponding here to an 18.8 nm oscillation amplitude i.e. a 0.84 V set point voltage). The relative position of the nanogear before and after the manipulation is given in Fig. 5a. The 300 nm lateral displacement of the piezo table was the same for all the z value selected. Notice that the piezo table was moved only in X direction to keep the deflection of the laser beam only in one direction to get the maximum sensitivity for the output signal.

When the tip apex is far away from the surface (z = - 8 nm to z = - 4 nm), the Fig. 5b oscillation amplitude along a line scan is corresponding to the awaited variation in a constant height mode. It decreases when the tip approaches and passes over the nanogear [19]. The corresponding Fig. 5c deflection signal does not show up any changes during a given scan, indicating that the tip apex was not in direct contact with the nanogear and that the cantilever was not bent. As the tip is brought closer to the sample surface (z = - 2 nm), the oscillation amplitude decreases slightly more as the tip passes over the nanogear. The deflection signal presents a small dip corresponding to an interaction increase with the top of the nanogear. This deflection can be interpreted as a small bending down of the cantilever due to the attractive interaction between the tip apex and the nanogear. In air, such an attractive interaction generally originates from surface contamination and from the thin water film present on the surface.

While approaching further the tip apex to the HOPG surface and reaching now z = 0, a saturation of the oscillation amplitude appears when the tip apex is in contact with the nanogear. Consequently, a bump now appears in the cantilever deflection signal during the piezo table

scan since the cantilever is now bending up [20]. When the tip apex and the HOPG surface are getting even closer (z = +2 nm to z = +4 nm), the amplitude oscillation saturation extends further during the piezo table scan. The deflection bump increases even more and the tip apex is pushing on the edge of the nanogear. The nanogear manipulation threshold is reached for z = +6 nm. Here, the oscillation amplitude signal fully saturates while scanning with the piezo table. After this manipulation at z = +6 nm, the AFM image was recorded by returning to a normal tapping imaging mode showing that the nanogear has been successfully moved laterally by less than 300 nm.

Figure 6 is also presenting the manipulation in a pushing mode of a 90 nm diameter nanogear (15 nm in thickness) up and down a native HOPG step of about 2.7 nm height i.e. 8 graphene layers in height (1 layer = 0.335 nm). This manipulation was accompanied by a rotation along the manipulation pathway. Notice as presented in Fig. 6b that the manipulation process using the piezo table is precise enough to position the nanogear well across the step edge. Without any apparent damage of the step edge and of the nanogear, one can manipulate the nanogear up and down this step edge indicating a rather smooth atomic scale border of the HOPG 8 layers step edge used. A 10 ML step edge will not allow such a manipulation and is used in the next section to construct a rack and pinion mechanism.

4. Simple mechanical experiments with a few solid state nanogears

With our actual process, below 100 nm in diameter and in absence of a central shaft, a nanogear does not have enough friction on the HOPG surface and in air to rotate around its center [7]. Hence and with their teeth intertwined, a combination of two 90 nm in diameter nanogears was used to assemble by AFM manipulation in a pushing mode a circular rack and pinion device. By using a very short manipulation sequence, one of the 2 nanogear was pushed and then rotates around the second one. Generally, such a manipulation leads to only a few 1/12 of a turn for a 6 teeth nanogear (see the sequence from Fig. 7c to 7d). A further push on a tooth drives the manipulated nanogear away from the supposed fixed one and leads to a set of entangled nanogears which can only be manipulated together with no control of their relative orientation.

To demonstrate how below 100 nm in diameter, a nanogear can be step by step rotate on the HOPG surface, we have used an HOPG native step edge to play the role of a rack in a rack and pinion mechanism. Using the Fig. 6 experimental results, we have first determined the tip apex

to surface distance and the minimum step height to avoid any jump of the manipulated nanogear over the step edge. The Fig. 7e to Fig. 7i tapping mode AFM images correspond to a manipulation sequence of a 90 nm in diameter nanogear with 6 teeth step by step rotated along a 3.1 ± 0.2 nm (10 ML) HOPG step edge playing here the role of a nano-rack. The nanogear was first brought in contact with the step edge to ensure a good interaction with one of its teeth (Fig. 7e). The AFM tip apex was positioned in contact with the tooth opposite to the one in interaction with the step edge. After approaching the AFM tip apex 12 nm towards the surface, the piezo table was moved as discussed in section 3 in such a way that the tip apex is pushing on a tooth in a direction parallel to the step edge. By pushing step by step on the nanogear teeth one after the other and in a direction parallel to the step edge, a rotation of the nanogear was observed along this step edge similar to a standard solid state gear rotating along its rack in a rack and pinion mechanical device. From Fig. 7e to Fig. 7i, 4 step by step rotations are presented in clockwise direction.

For a rigid body, the θ rotation angle (in degrees) of a disk of radius R on its support leads to a displacement $d_c = \frac{2\pi}{360} R\theta$ of its center of rotation. During the 1/12 turn of the 90 nm nanogear from Fig. 7e to Fig. 7f, its rotation center moved by $d_c = 30$ nm ± 3 nm indicating an effective nanogear rotation of $\theta = 38° \pm 2°$ during its displacement. The displacement of the nanogear center from Fig. 7f to 7g is $d_c = 29$ nm ± 3 nm, from Fig. 7g to 7h $d_c = 42$ nm ± 3 nm and from Fig. 7h to Fig. 7i, $d_c = 20$ nm ± 3 nm. The corresponding rotation angles are respectively $\theta = 27° \pm 2°$, $\theta = 32° \pm 2°$ and $\theta = 26° \pm 2°$ i.e. not exactly 1/12 of a turn per step. Around the expected 30° (1/12 of a turn according to the AFM images), the dispersion in θ is caused by the irregularity of the atomic scale structure of the step edge along the manipulation direction and also by the variations of the teeth length relative to the geometrical center of the nanogear. Furthermore, the 42 nm very long motion of the nanogear center from Fig. 7g to Fig. 7h also indicates a slipping motion probably due to a non-adapted pushing strength of the tip apex as a function of the step edge corrugation. In the prospect of a motion transmission to/from a solid state nanogear to a molecule-gears, the 3.1 ± 0.2 nm native corrugation of the HOPG step edge used is intermediate between the 2.0 nm height of a molecule-motor [8] and the actual 15 nm thickness of the solid state nanogears manipulated here.

5. Conclusion

A nanofabrication process was presented on an HOPG surface to produce a large number of solid state nanogears. The complete optimization of the nanofabrication process leads to the fabrication of 15 nm thick nanogears with a diameter down to 30 nm. Solid state nanogears down to 57 nm in diameter can be reproducibly manipulated in air by the tip apex of an AFM in a pushing mode. Native HOPG surface steps of at least 3.1 ± 0.2 nm in height can be used as a nanorack for those nanogears showing a nice gearing effect along the step edge. This points out that a minimum 3.1 ± 0.2 nm in height graphene nanogears will be able to gear with the 15 nm thick solid state nanogears studied here opening the way for a transmission of rotation between a molecule-gear and a solid state nanogears. Our nano-mechanics is still missing a technology to fabricate the nano-shaft, an important problem under exploration together with the compatibility of our nanofabrication process with nano-mechanical experiments in UHV conditions to be compatible with the environment of single molecule manipulations.

Acknowledgement: We like to thank the MANA-NIMS project and the A*STAR VIP Atom Tech program for the opportunity to explore single solid state nanogear mechanics.

References

[1] J. J. Uicker, G. R. Pennock, and J. E. Shigley, *"Theory of Machines and Mechanisms"*, Oxford University Press, New York, 2003

[2] E. J. Garcia and J. J. Sniegowski, Sensors & Actuators, **A48**, 203 (1995)

[3] J. J. Sniegowski and M. P. de Boer, Annu. Rev. Mater. Sci., **30**, 299 (2000)

[4] C. S. Ah, Y. J. Yun, H. J. Park, W. J. Kim, D. H. Ha, and W. S. Yun, Chem. Mater. **17**, 5558 (2005)

[5] Y. J. Yun, G. Park, C. S. Ah, H. J. Park, W. S. Yun, and D. H. Ha, Appl. Phys. Letts. **87**, 233110 (2005)

[6] Y. J. Yun, C. S. Ah, S. Kim, W. S. Yun, B. C. Park and D. H. Ha, Nanotechnology, **18**, 505304 (2007)

[7] J. Deng, C. Troadec, F. Ample, and C. Joachim, Nanotechnology, **22**, 275307 (2011).

[8] U.G.E. Perera et al., Nature Nanotechnology , **8**, 46 (2013).

[9] C. Bombis, et al., Phys. Rev. Lett., **104**, 185502 (2010).

[10] Manzano C, Soe W-H, Wong H S, Ample F, Gourdon A, Chandrasekhar N and Joachim C Nat. Mater., **8**, 576 (2009)

[11] T. Ondarçuhu, L. Nicu, S. Cholet, C. Bergaud, S. Gerdes, and C. Joachim, Rev. Sci. Instru. **71**, 2087 (2000)

[12] M. Urbakh, J. Klafter, D. Gourdon and J. Israelachvili, Nature, **430,** 525 (2004)

[13] D. W. Lee, X. Banquy and J. N. Israelachvili, PNAS, **110**, E567 (2013)

[14] V. N. Popok, I. Barke, E. E. B. Campbell and K. H. Meiwes-Broer, Surf. Sci. Reports, **66**, 347 (2011)

[15] P.M.I. Dinh, P.G. Reinhard and E. Suraud, Phys. Rep., **485**, 42 (2010)

[16] Y. Fakuma, T. Murakami, H. Asada, T. Koyanagi, Physica E, **10**, 273 (2001)

[17] X. Bouju, C. Joachim, and C. Girard, Phys. Rev. B., **59**, R7845 (1999)

[18] F. Moresco, G. Meyer, K. H. Rieder, H. Tang, A. Gourdon, and C. Joachim, Phys. Rev. Lett., **87**, 088302 (2001)

[19] R. Resch, A. Bugacov, C. Baur, B. E. Koel, A. madhukar, A. A. G. Requicha and P. Will, Appl. Phys. A., **67**, 265 (1998)

[20] A. Kühle, A.H. Sorensen, J. Bohr: J. Appl. Phys., **81**, 6562 (1997)

Figure captions

Figure 1. (a) The process flow for the fabrication of SiO_2 nanogears down to a 30 nm outer diameter with 6 teeth. A: the initial graphite substrate with its ultra-thin spin-coated HSQ layer. B: the e-beam lithography step where the nanogear size and shape are electronically exposed by scanning. C: after the HSQ processing (annealing, development), the amorphous SiO_2 nanogears remain on the graphite surface. (b) An SEM image of a large series of fabricated nanogears. Each set consists of 20 lines of nanogears. Per line, there are one 153 nm in diameter with 8 teeth and 5 different in diameter nanogears down to 30 nm with 6 teeth. Many nanogears below 57 nm in diameter are not respecting the e-beam pattern alignment.

Figure 2. The detail SEM and tapping mode AFM images of 2 nanogear lines fabricated on the HOPG surface. (a) An SEM image where the largest nanogears is 153 nm in diameter with 8 teeth, and the other 4 nanogears per line with 6 teeth are 110 nm, 90 nm, 74 nm and 57 nm in diameter respectively. (b) A tapping mode AFM image of the same two lines recorded with an oscillation amplitude set point of 0.47 V and an oscillation frequency of 321.6 kHz. The down-right largest nanogear seats on 3 native HOPG surface steps. (c) A scan line (solid line) crossing the center of the nanogear. The two higher steps underneath (marked step 2 and step 3) are still distinguished. The lateral dash line crossing over the 3 steps act as a reference scan profile of the HOPG surface for this peculiar step profile. Here, the 3 native steps (marked step 1, step 2 and step 3) are 1 nm, 3.1 nm, and 5.6 nm in height respectively.

Figure 3. (a) The minimum in diameter fabricated nanogear as a function of the specific HSQ layer thickness and dilution used in the process. From (b) to (f): the corresponding SEM images with diameter (b) 30 nm for 15 nm HSQ, (c) 48 nm for 30 nm HSQ, (d) 58 nm for 50 nm HSQ, (e) 60 nm for 60 nm HSQ and (f) 60 nm for a 90 nm thick HSQ layer. To expect to go down in diameter limit, a new graph will have to be plotted for another resist (if it exists) for a new de-wetting limit

Figure 4. Two sequences of a single 90 nm nanogear manipulation with AFM tip by moving the piezo table opposite to the displacement direction. Tapping mode AFM images: (a) before, (b) after the first, and (c) after the second manipulation at a 1.22 V oscillation amplitude set point and a 321.6 kHz oscillation frequency. The dotted stars superimposed on these images

indicate the nanogear locations before each manipulation; the short dash lines crossing the nanogear center direct the orientations; the crosses are marking the tip positions before the manipulation and the arrows indicate the manipulation directions. (d) The recorded oscillation amplitude signals during the first (solid line) and second (dash line) nanogear manipulation. Timing: T_1: the feedback loop is turned off, T_2: the tip apex is approached towards the surface by 12 nm, T_3: the tip apex is in interaction with the nanogear, T_4: the tip apex is in mechanical contact with the nanogear and T_5: the manipulation is finished. During the time interval T_4 – T_5, the oscillation amplitude is characteristics of the nanogear manipulation. (e) The cantilever deflection recorded following the same time sequence.

Figure 5. Variations of the cantilever oscillation amplitude and deflection for different tip-surface distances while moving the piezo table instead of scanning the AFM tip. Tapping AFM images (a) before and (b) after the nanogear manipulation. The dash line in (a) is the trace of the tip scanning over the nanogear. The crosses mark the tip positions before (left) and after (right) the line scans. The white dotted star shows the nanogear location before the manipulation. (c) The cantilever oscillation amplitude recorded during the piezo table motion at the different tip-surface distance. z = 0 is the reference tip-surface distance at a 0.84 V oscillation amplitude voltage set point (18.8 nm oscillation amplitude). The first saturation at z = - 2 nm is characteristic of a tip apex to nanogear contact. (d) The corresponding cantilever deflection recorded during the same piezo table motion.

Figure 6. A series of tapping mode AFM images to follow the step by step manipulation of a nanogear across a 3.1 nm height HOPG surface step (oscillation amplitude voltage set point: 0.65 V; oscillation frequency: 321.6 kHz). (a) to (c) the nanogear was manipulated down the step. (d) to (f) the nanogear was manipulated up the same step. The crosses indicate the tip apex positions before the manipulation and the arrows show the manipulation directions opposite to the directions of the piezo table displacements.

Figure 7. Two series of a single nanogear rotation. From (a) to (d), the top nanogear marked by a white arrow was pushed towards the down nanogear and step by step pushed around it. From (b) to (c), a first 1/12 (30°) of a turn was obtained with the down nanogear preserving its position. From (c) to (d), 1/6 of a turn was obtained for the top nanogear. At the same time, the down nanogear moved down by 42 nm and turn in counterclockwise direction by 21°. By pushing again on the top nanogear, both nanogears move following the (c) to (d) sequence

before forming one single object (AFM images recorded at a 0.64 V oscillation amplitude set point). From (e) to (i), the nanogear marked by the white arrow was anchored down to a 3.1 nm height native HOPG surface step edge and then step by step rotated clockwise along this step edge. From (e) to (f): one tooth is interacting with the step edge and then the tip apex displaced the nanogear center by 30 nm equivalent to about 1/12 turn. As a consequence, 2 teeth are now interacting with the step edge in (f). A 29 nm displacement was obtained from (f) to (g) with a consequent 27° clockwise rotation, a 42 nm displacement with a 32° clockwise rotation from (g) to (h) and a 20 nm displacement with a 26° clockwise rotation from (h) to (i). The short dash lines direct the nanogear orientation starting from the perpendicular to the step edge orientation in (e). The AFM images (e) - (i) recorded at a 1.22 V oscillation amplitude set point.

Figure 1

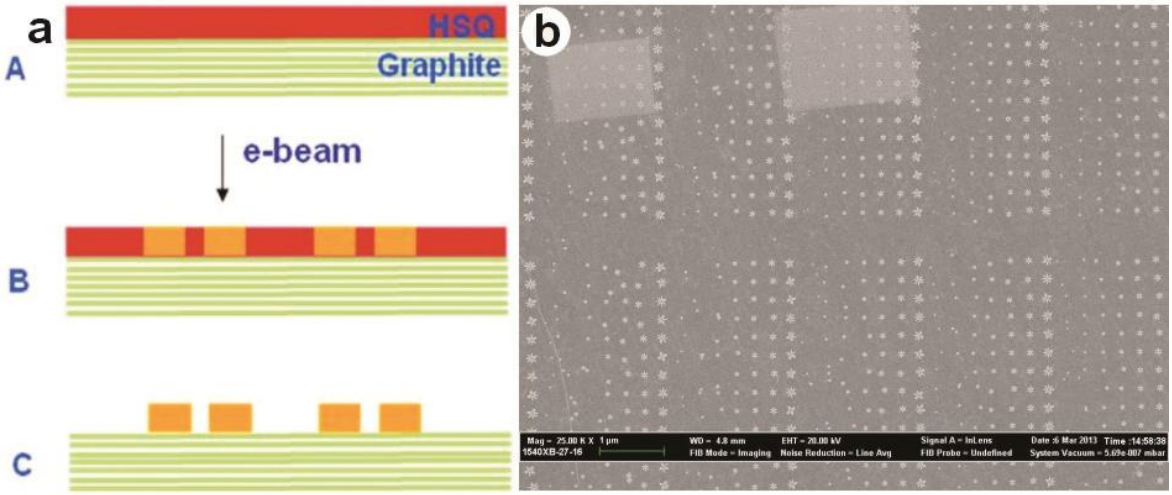

Figure 2

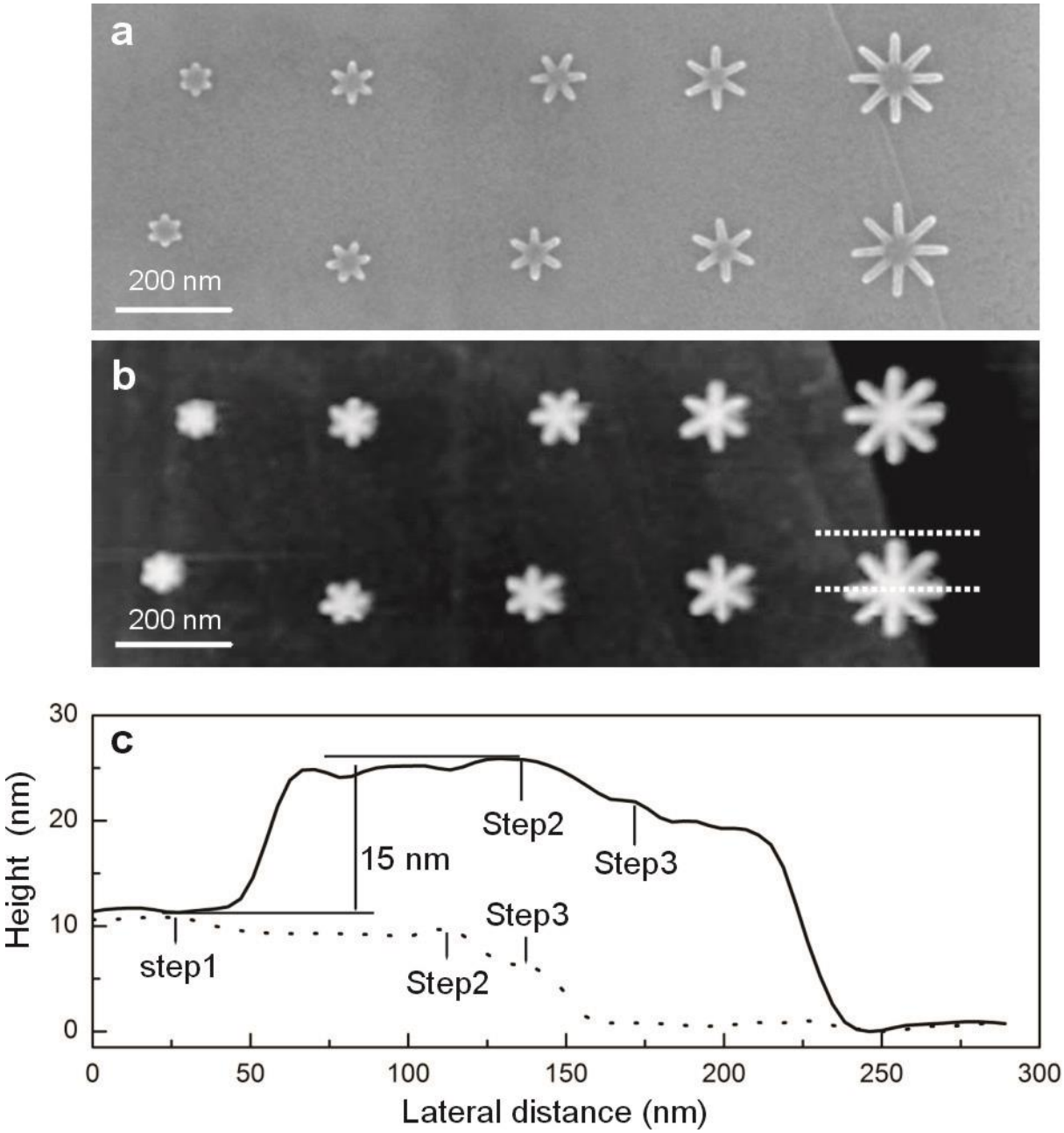
a
200 nm
b
200 nm
c
Height (nm)
Lateral distance (nm)
15 nm
Step2
Step3
Step3
step1
Step2
0
10
20
30
0
50
100
150
200
250
300

Figure 3

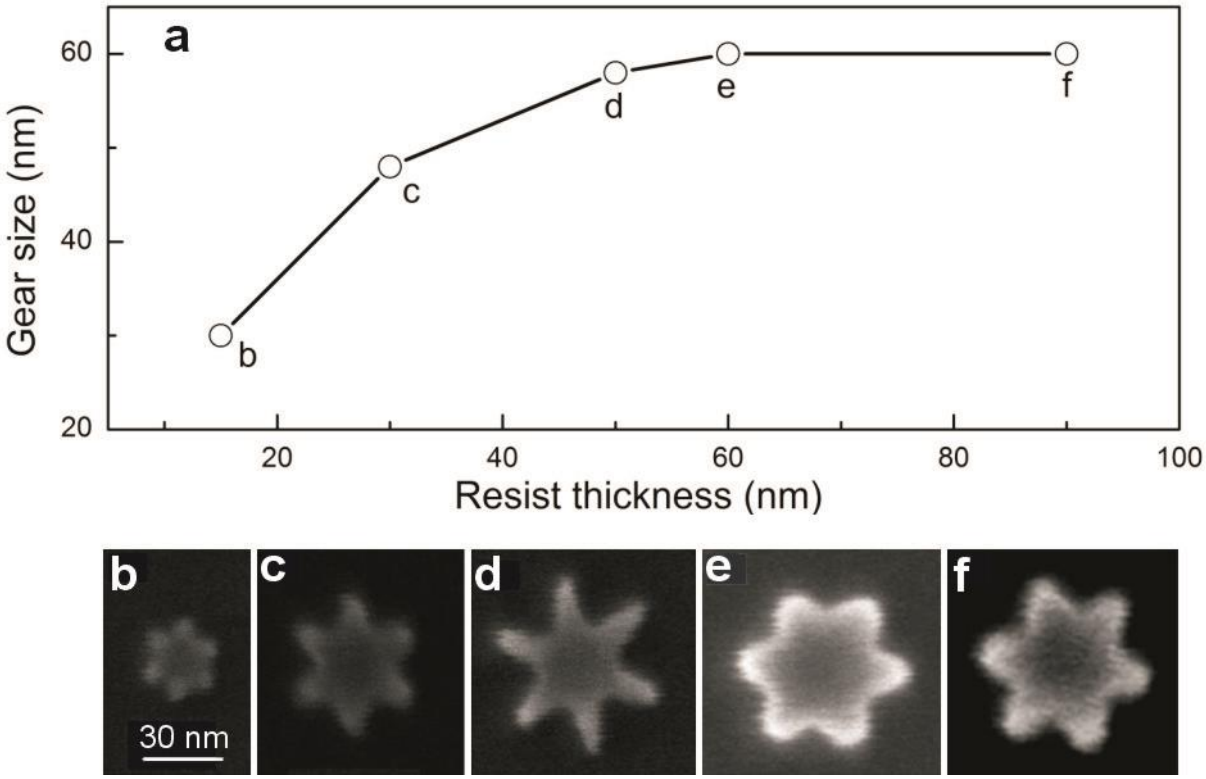

Figure 4

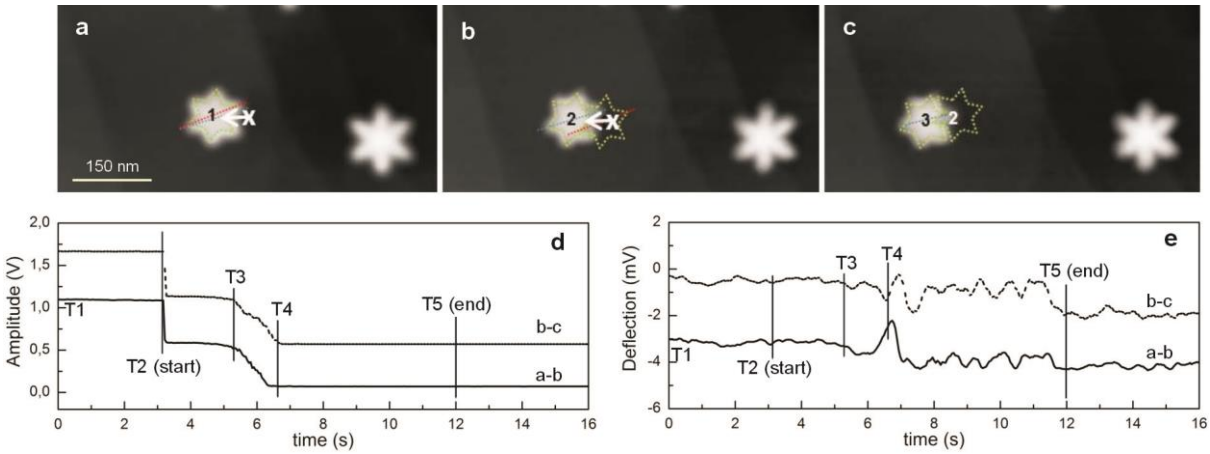
a
b
c
1
2
3
150 nm
d
Amplitude (V)
T1
T2 (start)
T3
T4
T5 (end)
b-c
a-b
time (s)
e
Deflection (mV)
T1
T2 (start)
T3
T4
T5 (end)
b-c
a-b
time (s)

Figure 5

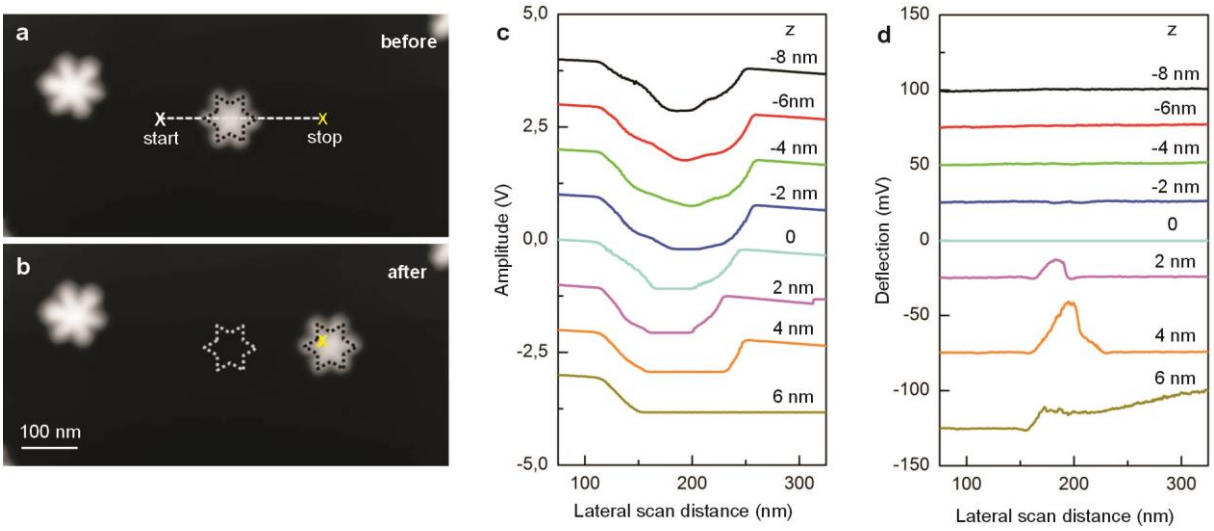
a
before
start
stop
b
after
100 nm
c
z
-8 nm
-6nm
-4 nm
-2 nm
0
2 nm
4 nm
6 nm
Amplitude (V)
5,0
2,5
0,0
-2,5
-5,0
100
200
300
Lateral scan distance (nm)
d
z
-8 nm
-6nm
-4 nm
-2 nm
0
2 nm
4 nm
6 nm
Deflection (mV)
150
100
50
0
-50
-100
-150
100
200
300
Lateral scan distance (nm)

Figure 6

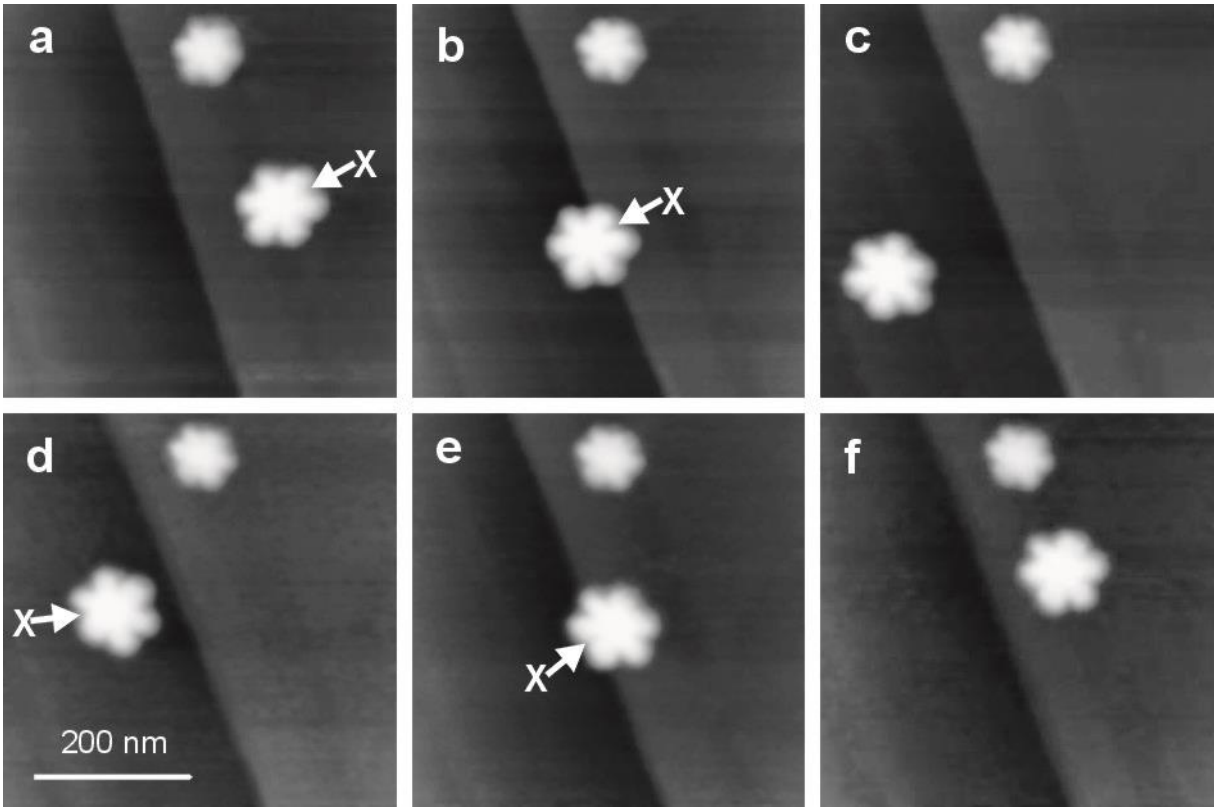

Figure 7